Magazine of Civil Engineering

ISSN 2712-8172

journal homepage: http://engstroy.spbstu.ru/

Research article

UDC 69

DOI: 10.34910/MCE.128.8

Influence of silica fume addition on enhancing the autoclaved aerated concrete properties

R. Shabbar ✉, ***L.A.M. Alasadi, J.K. Taher***

University of Kufa, Najaf, Iraq

✉ *rana.shubber@uokufa.edu.iq*

Keywords: autoclaved aerated concrete, modified AAC mix, waste material, water absorption coefficient

Abstract. The demand for lightweight concrete has increased because of its low density, fire resistance and good thermal insulation. Autoclaved aerated concrete (AAC) is the combination of cement, fine-grained sand, lime and water with aluminium powder. This study aims to investigate the influence of adding silica fume (SF) on improving the properties of AAC. The response was studied in terms of testing the mechanical and physical properties including compressive, splitting tensile, flexural strength, density, porosity and coefficient of water absorption. Different mixes have been proposed by incorporating the SF with contents of 10 %, 20 % and 30 % by cement weight, which is compared with the AAC sample that is used in practical applications. The results indicated that there was a significant improvement in the compressive and flexural strength of AAC, which increased by six and three times, respectively, when 30 % of SF was used with an acceptable dry density. Furthermore, the microstructural analysis revealed that SF had a positive effect on the development of calcium silicate hydrate and it can be used in AAC masonry block productions.

Acknowledgements: The authors are grateful to MSc. Abbas Diwan, a researcher at the Nanotechnology and advanced Materials Research Unit, and to MSc. Mohammed Madlool, Materials Engineering Department, Faculty of Engineering, University of Kufa, for their support in preparing the tests.

Citation: Shabbar, R., Alasadi, L.A.M., Taher, J.K. Influence of silica fume addition on enhancing the autoclaved aerated concrete properties. Magazine of Civil Engineering. 2024. 17(4). Article no. 12808. DOI: 10.34910/MCE.128.8

1. Introduction

In the last two decades, much attention has been paid to the production of lightweight concrete (LWC) due to its low density, good thermal insulation and fire resistance, lower thermal conductivity and shrinkage with a fast construction process [1, 2]. In addition, the use of LWC increases the building's resistance to seismic loads and decreases operating and construction costs. Thus, it is used in a number of applications over normal concretes [3, 4]. Generally, LWC is divided into lightweight aggregate concrete (LWAC), in which light coarse aggregate is used, and aerated concrete (AC), which is produced using cement mortar with some foaming agent or void-forming materials without coarse aggregate [5, 6].

Several researchers have investigated the physical and mechanical characteristics of AC with using an autoclave. Sufficient autoclave curing results in the crystallization of calcium silicate hydrate (CSH) and neutral tobermorite-11, the main structural minerals of autoclaved aerated concrete (AAC). The tobermorite phase begins after 2 h of autoclaving and lasts up to 8 h. Wang et al. [7] realised that an extreme prolongation of autoclaving did not affect the formation of tobermorite. In contrast, Mostafa [8] observed that compressive strength enhanced during the first 6 h of autoclaving, and then the gain in strength declined at 12 h and 24 h. Kunchariyakun et al. [9] reported that the compressive strength in the range of 20–60 % was lower than the strength of the control samples, while the unit weight loss was in the range of 16–45 % for the samples that were subject to autoclave curing. In addition, the highly reactive silica in rice

husk ash (RHA) affected the transformation of tobermorite and the increasing the autoclaving time to 18 h had no major effect on the properties of AAC. Cai et al. [10] studied the effect of iron tailings content and fineness on mechanical properties of AAC. The mass ratio of iron tailing to silicon sand (MSIS) were 0 %, 20 %, 40 %, 50 %, 60 %, 80 % and 100 % with a grinding time prolonged from 10 to 30 mins. It is indicated that the compressive strength reduced by 21 % with the increase of MSIS up to 50 %, while it dropped by 48 % with the increase of MSIS up to 100 %. It was reported that the optimal grinding time was 20 min. Cai et al. [11] investigated the influence of waste materials on high content solid-wastes autoclaved aerated concrete (HCS-AAC) performance. The results exhibited that the grinding process had a significant influence on the powder particle size and the compressive strength obtained from mix grinding increased by 3–6 %.

Wongkeo et al. [12] studied the flexural strength, compressive strength and thermal conductivity of AAC by replacing cement with bottom ash (BA) up to 30 % by weight. The results exhibited that the flexural strength, compressive strength and thermal conductivity increased with increasing BA content. The 20 % increase in both compressive and flexural strengths was found for mixes with 30 % BA content compared to the mixes without BA content, whereas the thermal conductivity improved only by 6 %. Różycka and Pichór [13] utilized perlite waste as a quartz sand replacement in conventional AAC mixtures at 5 %, 10 %, 20 %, 30 % and 40 % by weight. The results showed that the bulk density decreased by 12 %, compressive strength by 9 % and thermal conductivity by 10 % with 5 % of perlite waste. Gunasekaran et al. [14] studied the effect of natural sand replacement by flash ash (FA) up to 100 %. The results indicated that compressive strength, dry density and water absorption declined with adding FA. The maximum values were with 0 % FA that was greater than with 100 % FA by 53 %, 33 % and 22 % respectively. Furthermore, Qin and Gao [15] used the recycling of waste autoclaved aerated concrete (WAAC) powder with cement by accelerated carbonation. Carbonation curing was achieved on a cement paste containing up to 50 % of WAAC powder. The result revealed the highest compressive strength was obtained with the optimal dosage of WAAC of 20 % that was enhanced by 2 %.

However, Li et al. [16] used the municipal solid waste incineration (MSWI) bottom ash as a sand replacement in AAC. The results showed that MSWI caused a reduction in compressive strength, density and thermal conductivity with increasing its content. The lowest value was with 100 % replacement, which caused a decrease in compressive strength, density and thermal conductivity by 71 %, 9 % and 17 % respectively. Kunchariyakun et al. [17] studied the impact of black rice husk ash (BRHA) and bagasse ash (BA) on the dry density and compressive strength of AAC at 180 °C for 4, 8 and 12 h. Sand with the range of 0 %, 30 % and 50 % by weight was replaced with BRHA and BA. The results showed that an increase in curing time has an obvious effect on the compressive strength of AAC which improved by 46.59 % and 26.97 % in samples containing 30 % of BA and 30 % of BRHA respectively. However, no significant effect on the dry density developed by 9 % and 10 % with the optimum time of 12 h has been reported. In addition, Zafar et al. [18] used waste granite dust (WGD) as a sand replacement for up to 20 %. The results revealed that the maximum increase in the hardened density, thermal conductivity, compressive and flexural strength is higher with 20 % of WGD than 0 % of WGD by 13.45 %, 36 %, 42 % and 38 % respectively, while the minimum water absorption was lower with 20 % by 26.7 %.

The influence of pozzolanic materials such as silica fume (SF), granulated blast furnace slag (GBFS) and fly ash (FA) on the AAC properties considers an essential issue on its behavior analysis [19]. Pehlivanlı et al. [20, 21] investigated the impact of four different types of fibers (polypropylene, carbon, basalt and glass fiber) on the compressive and flexural strength of AAC. The results indicated that carbon fiber-reinforced AAC, as opposed to other types of fibers, provided the greatest compressive and flexural strength, which increased by 31 % and 61 % respectively. In Güçlüer et al. [22] siliceous aggregate was replaced by fly ash and silica fume was added with the range of 3 %, 6 %, 9 % and 12 % to the cement. Results showed that curing under 177 °C had a greater compressive strength than at 156 °C, which improved by 78 % with SF of 3 %.

Chen et al. [19] studied the effects of silica-lime-cement composition on the density and compressive strength. Lime (L) and cement (C) were used with a range between 5 % and 30 %, while SF was from 60 % to 70 % and aluminium powder from 0.25 % to 1 %. It was revealed that samples with 70 % of SF, 25 % of L and 5 % of C had the highest strength and density. The increase in the compressive strength was related not only to the progress of hydration reactions, but also to pores filling with the hydration products. On the other hand, the effects of SF and steel slag additions on compressive strength and thermal properties of lime-fly ash pastes were studied by Zhao et al. [23]. Curing conditions of 180 °C for 8 h and SF content of 8 % and 15 % of SF was adopted. SF caused a significant development in compressive strength, which raised by 59.6 % with 15 % of SF. Leonteva et al. [24] considered the influence of ultra- and nanodisperse size of silica gel content in the range between 4 % and10 % additives on the structure and mechanical-and-physical properties of heat insulating AAC. The results showed that the compressive strength increased 5 times, when using silica up to 10 % with a slightly improved dry density of 6.5 %. Pachideh et al. [25] adopted SF with 7 %, 14 % and 21 % of cement weight. They confirmed that the compressive and

tensile strength enhanced by 63 % and 23 % when 21 % and 7 % of SF respectively were used, while water absorption decreased with increasing SF content up to 21 % which decreased 2 times at 10 and 30 and 21 % at 90 min. Almajeed and Turki [26] used SF with a maximum value of 16 %. They observed that the compressive strength developed up to 23 % with 12 % of SF.

Lashari et al. [27] studied the effect of SF and FA as cementitious materials on the properties of the AAC. SF was substituted up to 20 %. Then FA was replaced with cement up to 30 % after selecting the optimum contain of the SF. It is indicated that the greatest split tensile and compressive strength of the AAC was when cement was replaced by 15 % of SF and 30 % of FA.

It is known that the use of AAC blocks has increased dramatically throughout the world due to several advantages of such blocks, including their light weight, thermal insulation and cost-effectiveness. However, low mechanical properties and problems with the durability of such blocks limit their use, for example, for filling the walls of internal partitions of multi-story buildings. This study aims to improve the mechanical properties (compressive, tensile and flexural strengths) of the non-structural AAC blocks to be used in the construction of load-bearing walls and reduce the cracking shrinkage resulting from dimensional changes caused by environmental humidity. A modified mix with different contents of SF (10 %, 20 % and 30 %) and reduced sand and water content was proposed to reduce the size of voids in the mix.

2. Methods and Materials

2.1. Material Properties for the AAC Mix Design

The ACC mixture prepared during this study consists of the following components:

- Ordinary Portland Cement CEM I/42.5N that satisfies the requirements of the Iraqi Organization of Standards (IOS.5/1984 [28]);
- sand with particle size distribution between 1 and 3 mm [29];
- ECA MICROSILICA-D [30] with an average diameter of 0.15 μ;
- lime (CaO), approximately 90 % of which can pass through the sieve 90 μm [31].

To produce AAC samples, aluminium powder with a purity of 90 % was used. The chemical, physical and mechanical properties of the OPC are revealed in Tables 1, 2 and 3. Whereas, the properties of lime and silica fume which were used in the mixtures are shown in Tables 4 and 5 respectively.

Table 1. Chemical properties of Ordinary Portland Cement.

Component	Test result, %	IOS.5/1984
SiO_2	20.35	-
Al_2O_3	5.71	-
Fe_2O_3	3.46	-
CaO	61.93	-
MgO	3.78	Max. 5.0
SO_3	2.39	Max. 2.8
Loss on ignition	1.51	Max. 4.0
Insoluble residue	0.52	Max. 1.5

Table 2. Physical properties of Ordinary Portland Cement.

		Test result	IOS.5/1984
Setting time	Initial (min)	110	Min. 45
	Final (hr)	2.76	Min. 10
Fineness		2795	Min. 2300

Table 3. Mechanical properties of Ordinary Portland Cement.

Mechanical	Compressive strength	3 days	22.3 MPa	Min. 15
		7 days	32.3 MPa	Min. 23
Soundness, %		0.31	0.32	
Residue, %	90	6.08	6.08	
	180	0.58	0.58	

Table 4. Lime properties.

Properties	Test result	IOS.807/1988
Extinguishing time (min)	13	5-15
Activity CaO, %	91.97	Min. 85
CO_2	1.46	Max. 5
Fineness (remaining on sieve 90 μ), %	1	Max. 10

Table 5. ECA MICROSILICA-D Silica Fume properties [30]

Properties	Test result	ACI 234R-96 [32]
Specific Gravity	2.25±15 % at 20°C	2.2 %
Sulphate Content	1.0 % as SO_3	≤ 4 %
Bulk Density	≥550 kg/m^3	480–720 kg/m^3
SiO_2 Content	90 %	84–91 %

2.2. Preparation of Samples

To produce a slurry, sand was mixed with one-third of water for nearly 1.5 min. Then, cement and lime were added to the slurry and mixed for 100 sec. The remaining water was mixed with silica fume and aluminium powder for 80 sec. Then, all materials were mixed and the mixing process was completed within 50–60 sec. After that, the molds were heated to 42 °C and filled with fresh AAC. The samples were demolded for approximately 24 h, as shown in Fig. 1 [18]. The samples were cured under high-pressure steam conditions of 12 bars for 10 h at 190 °C and were left in the open air for 7 days. Then the AAC samples were tested for physical and mechanical properties with microstructural fracture surface.

(a) Samples after casting **(b) Samples volume after expansion**

Figure 1. AAC samples with different silica fume content: cubes, beams and cylinders.

2.3. Mechanical and Physical Tests

The compression test was achieved using 100 mm cubes according to BS EN 679 [33], whereas the splitting test has been conducted using a cylinder of 100 mm diameter and 200 mm height according to BS EN 1881-117 [34], as indicated in Fig. 2 and 3. Flexural strength has been measured by using a prism with dimensions of 100 × 100 × 400 mm according to BS EN 1351 [35], as indicated in Fig. 4. However, bulk density was measured using a cylinder of 100 mm diameter and 70±5 mm height according to BS EN 678 [36]. Four values of SF (%) have been considered. Three samples were tested and the average value was adopted. For the industrial (control) and AAC, three samples were prepared.

As for porosity, it is defined as the ratio of the pore volume filled following a 30-min soak. After the samples had been dried to a constant weight, they were weighed (W_d). Then the samples were immersed in water for 30±0.5 min and the amount of water absorbed was weighted (W_s). The porosity was calculated using (1) [37].

$$P = \frac{(W_s - W_d)}{W_d} \times 100. \quad (1)$$

Figure 2. AAC cube for compressive strength test.

Figure 3. AAC cylinder for tensile strength test.

Figure 4. AAC prism for flexural strength test.

However, the coefficient of water absorption C_w detects the capability of material absorbing water through a cross-section area in the stated time according to BS EN 772-11 [38]. After the dry mass of the samples had been recorded, the samples were immersed in water (t_{so}) to a depth of 5±1 mm for 10, 30 and 90 min. Then each sample has been weighed as a mass of saturated surface. The water absorption coefficient was calculated using (2) [39].

$$C_w = \frac{W_{sat} - W_{dry}}{A_s \sqrt{t_{so}}} \times 10^6 \left[g \Big/ \left(mm^2 \times t^{0.5} \right) \right]. \quad (2)$$

2.4. Mix design

The mix proportion of the AAC containing different percentages of SF is shown in Table 6. For the industrial AAC, two parts of sand screened (0–3 mm) to one part of cement and 33 % lime with 0.32 % aluminium powder were used. However, for the proposed AAC, 2.6 of sand to 52 % lime with 0.21 % of aluminium powder were used. SF was inserted with 10 %, 20 % and 30 % by cement weight.

Table 6. Mix proportions for industrial and proposed AAC (kg/m³).

Material, kg/m³	Industrial (Control) sample	0 % SFAAC	10 % SFAAC	20 % SFAAC	30 % SFAAC
Cement	139	145	145	145	145
Sand	278	387	387	387	387
Water	463	220	220	220	220
Lime	46	75	75	75	75
AL powder	0.45	0.31	0.31	0.31	0.31
Silica fume (SF)	-	0	14.5	29	43.5

2.5. Optical microscope observations

The cross-section images of the AAC sample were captured by using an advanced metallurgical microscope, as shown in Fig. 5. It is a manual microscope, which is manufactured by KJ Group. Model EQ-MM500T-USB with 5.0 MP resolution was used to disclose the detailed microstructure of the samples. AAC with greater SF content exposed the lower number and non-uniform shapes of pores.

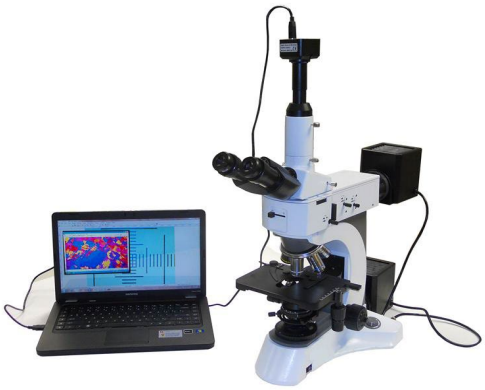

Figure 5. Advanced Metallurgical Microscope [40].

3. Results and Discussion

3.1. Compressive Strength

The compressive strength of AAC containing different SF percentages is shown in Fig. 6. The results indicated that compressive strength of the industrial (control) samples was lower than the experimental AAC without SF by 123 %, which may be due to its high water/cement ratio and aluminium powder content. Moreover, the space occupied by the hydration product improved due to an increase in water content, while the hydration volume remained constant regardless of the mixture's water content at a certain degree of hydration. It is unsure that an increase in water to water-to-cement ratio causes a rise in capillary voids and gel pores which was agreed with Naik [41].

The results showed that the strength of AAC increased with an increase in the proportion of SF. For the samples with 10 % and 20 % of SF, the compressive strength was higher than that of the control sample. However, the maximum strength was obtained at 30 % of SF, which was six times higher than that of the control sample. This behavior may be due to the effects of fine particle size of silica and large surface area consisting mainly of amorphous silicon dioxide. In addition, the formation of non-crystalline and crystalline CSH under autoclaving conditions was due to the reactions between reactive silica and lime [42], as shown in (3) and (4) [1]. The compressive strengths of the AAC samples were within the requirements of ASTM-C1693, which specifies the compressive strength of AACs from 2 to 6 MPa [43].

$$SiO_2 + CaO \xrightarrow{\text{Slag}} \alpha - C_2SH + C - S - H \longrightarrow \text{Tobermorite} \quad (3)$$

$$SiO_2 + CaO \xrightarrow{\text{Silica Fume}} C - S - H \longrightarrow \text{Tobermorite} \quad (4)$$

It was noted that the increase in the amount of waste materials resulted in an increase in the AAC strength, which is consistent with the other researches. Similar behaviors were reported in [18, 26, 44, 45]. Additional CSH gels occurred due to the reactions between free cement (created from cement hydration) and waste materials such as sawing mud, silica fume, granulated blast-furnace slag and WGD respectively, which caused a high compressive strength. It is expected that adding excess SF to AAC could increase the strength and durability of cementitious material with a slight increase in its weight.

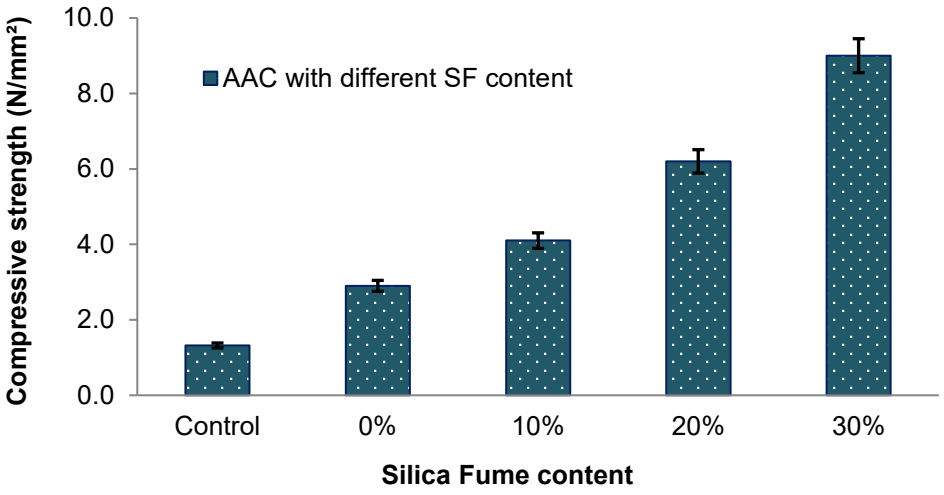

Figure 6. Compressive strength for the control and experimental AAC samples.

3.2. Tensile Strength

The tensile strength test results with different SF content are shown in Figure 7. The tensile strength of the control sample was higher than that with SF by up to 20 %. It was observed that the strength of the control sample was higher than that with 0 % SFAAC by 44 %. It could be referred to its high cement/sand ratio, which was ½ that appears to be adequate in providing a good tensile strength. However, the strength of the laboratory AAC mix increased with increasing SF content. At 10 % of SF, tensile strength increased by 38 % over 0 % of SF, followed by 52 % for 20 % of SF and the highest strength was achieved at 92 % by increasing SF to 30 % by weight. Based on the above results, when the addition of SF exceeds this limit, it is expected that higher tensile strength may be obtained. In addition, the tensile strength of 30 % SFAAC was slightly higher than that of the control sample by 7 %. This is in contrast with Toutanji et al. and Pachideh and Gholhaki results [25, 46], where SF was used in the range of (8-25) % and (7-21) % respectively. The results showed that the tensile strength increased slightly by 3 % when up to 8 % of SF was added, then it declined with increasing SF content, also the tensile strength increased by 23 %, when 7 % of SF was used [44, 46].

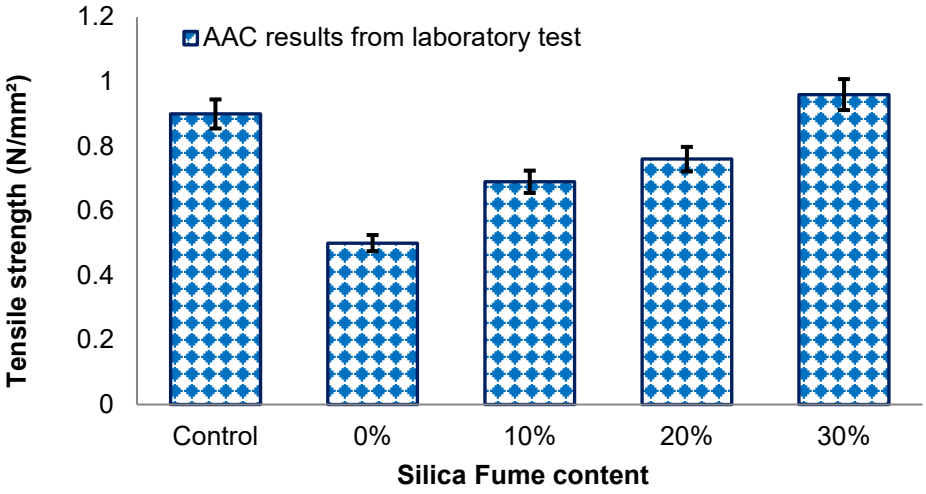

Figure 7. Tensile strength for the control and experimental AAC samples.

3.3. Flexural Strength

The results showed that all values of the AAC with SF were higher than that of the control sample, as shown in Fig. 8. In addition, the SF had a more prominent effect on flexural strength than on the splitting tensile strength, and for a high percentage significantly improved in strength, which agrees with [44]. The lowest value of the flexural strength was for control sample, which increased significantly by 122 % for 0 % SFAAC due to its high water/cement ratio. The presence of SF increased the flexural strength of AAC at 10 %, 20 % and 30 % of SF content by 1.6, 2 and 2.7 times, respectively. This behavior may refer to the further reaction of SF with $Ca(OH)_2$ obtained during Portland Cement hydration and create more CSH gels, which increase the strength of AAC. The optimal strength of mixes with SF was obtained for 30 % SFAAC.

In [12] similar behavior was observed, when BA was used as cement replacement in the range of 10–30 %. The flexural strength improved with increasing BA replacement and approximately 20 % increase in strength was obtained for mix with 30 % BA. However, in [40] SF with a range of up to 25 % was used. The result showed that maximum strength was obtained by replacing cement with 15 % of SF.

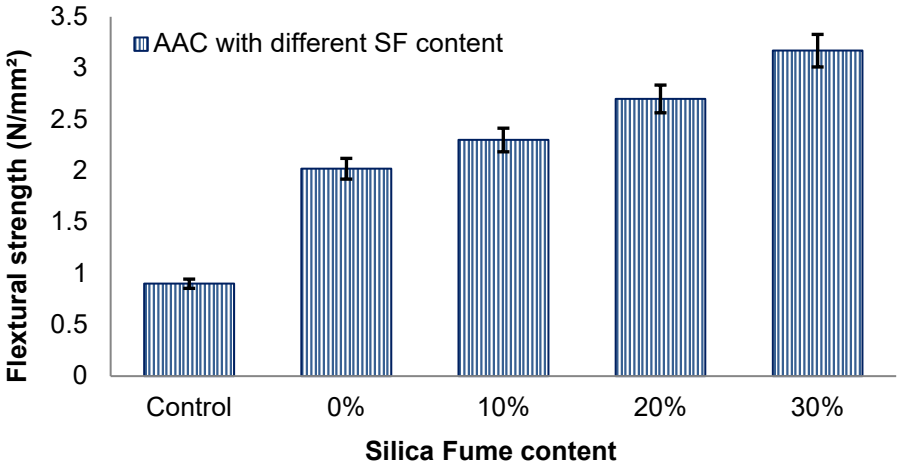

Figure 8. Flexural strength for the control and experimental AAC samples.

3.4. Bulk Density

Bulk density is one of the most important properties of AAC, and the mechanical and physical properties of AAC depend on their density and materials properties [13]. Fig. 9 shows the density of AAC with different SF content. The results showed that the density of AAC samples increased with the addition of SF, and the lowest value was for control sample, which improved by 28 % for 0 % SFAAC. With 10 % of SF, the bulk density increased by 44 %, followed by 46 % and 54 % for 20 % SFAAC and 30 % SFAAC, respectively. It could be due to the reactivity of the finer SF grain size, resulting in hardening AAC density. Moreover, the hydration process was accelerated by siliceous properties of waste materials by increasing the CSH content, resulting in a denser microstructure, which is consistent with [18, 47], where SF and WGD were used, respectively. The results showed that high density tobermorite crystals were formed with increasing waste materials content. In [26] it was observed that the dry density of AAC was not affected by the addition of SF due to its low content compared to the total amount of the mix.

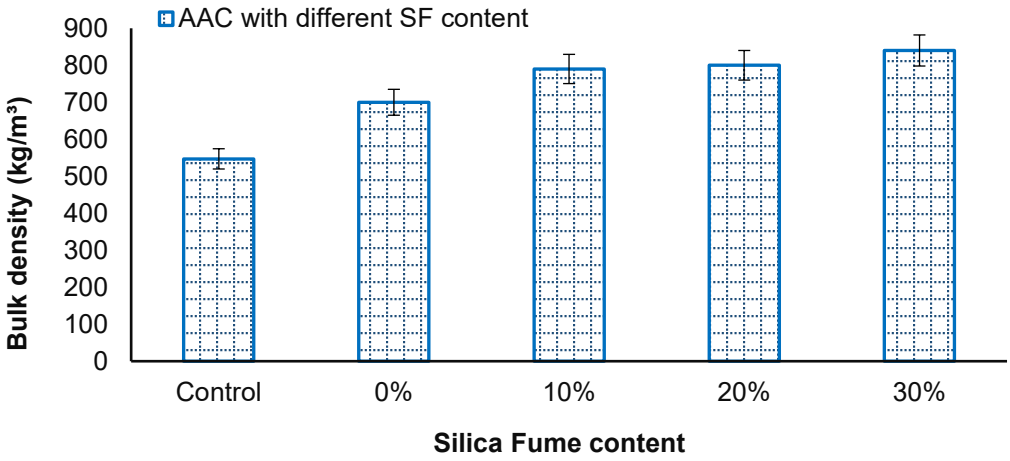

Figure 9. Dry density for the control and experimental AAC samples.

3.5. Porosity Measurement

AAC has a high porosity of more than 70 % of hardened material/volume, which leads to low compressive strength and density compared to conventional concrete [48].

The pore size distribution and porosity of AC are different and depend on the method of curing and materials composition. An increase in the volume of macropores led to an increase in porosity, which leads to thinning of the pore walls, thereby reducing the micropore volume of AC [49]. The results of the porosity of the control and proposed AAC samples with different SF content are shown in Fig. 10. The decrease in porosity with increasing SF content is neglected. The highest value was for control sample, which was

higher than 0 % SFAAC by 8 %, followed by 4.5 % and 2 %, when SF increased up to 30 %, which is consistent with [50]. When lightweight concrete (LWC) with different nanosilica content had similar porosity and NS1 (with 1 % cement replacement) showed lower porosity, which was reduced by 15 % compared to the control sample.

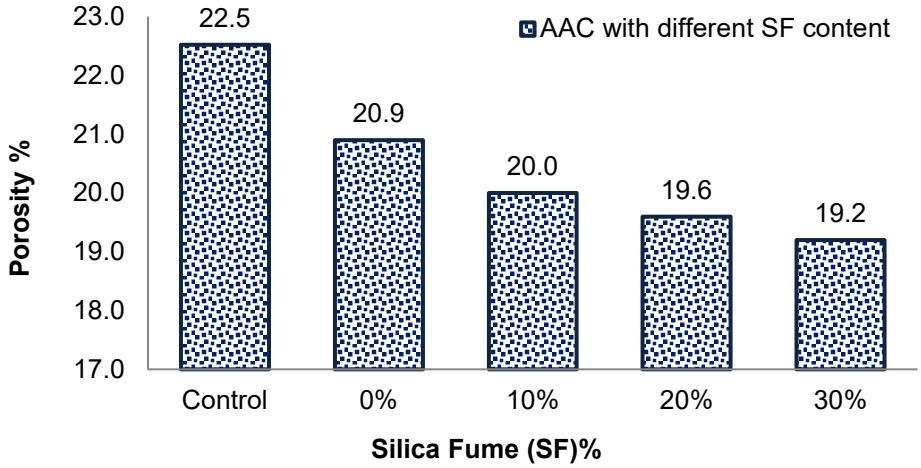

Figure 10. Porosity for the control and experimental AAC samples.

3.6. Coefficient of Water Absorption

Aerated concrete blocks have high water absorption and this problem needs to be solved. Fig. 11 shows the water absorption coefficients of the control and proposed AAC mixes at different times, including different SF content. It can be observed that all samples showed an increase in water absorption after 10, 30 and 90 min. After 10 min, the water absorption of the modified AAC samples with modified SF content was negligible. The highest value had the control sample, which may be due to its high aluminium content that caused a large number of voids.

After 30 min the water absorption for all experimental samples was the same, whereas after 90 min it was greater than that without silica and 30 % SF. Water absorption decreased with the addition of more SF content, which may be due to the fineness of void-filling particles and the cellular structure of AAC. This could be attributed to the plugging of connected pores by the microstructure densification due to the tobermorite formation and nano-micro-filling of voids. The capillary absorption mechanism of AAC is still unclear and its behavior depends on the features of the surrounding mortar, aggregate type and test conditions.

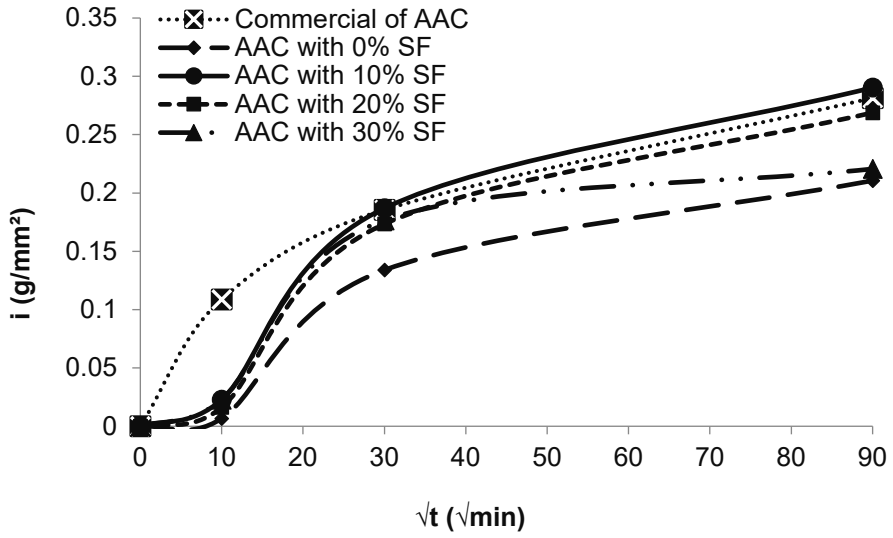

Figure 11. Water absorption for the control and experimental AAC samples.

3.7. Microstructural analysis

The microstructure of the AAC depends on many factors such as materials composition, type and amount, hydration rate and type of reaction produced and their distribution [9, 13]. However, the distribution of the micropore is more sensitive to the hydrothermal reaction [50]. The microstructures of the SFAAC and

the control samples were examined using advanced metallurgical microscope, and the results of this examination are shown in Fig. 12. Fig. 12a shows the high rate of macro- and micropores and subsequent tobermorite due to its high water/cement ratio. It resulted in an improvement in the hydration products formed and caused swells in the CSH gel and pore size became less than before. 0 % SFAAC had a higher rate of macropore volume, which tend to remain isolated as shown in Fig. 12b. This behavior may be due to intense reaction of silica with calcium hydroxide to form calcium silicate hydrates as indicated in (5) [51].

$$(C3S + C2S) + S \rightarrow CSH + CH + S\ (silica) \rightarrow CSH \rightarrow tobermorite \quad (5)$$

AAC with 10 %SF was more stable to conglomerate than to stay isolated because it had high pore volumes (Fig. 12c) and more tobermorite platelets were created, when there was enough silica in the mix. Moreover, an increase in SF to 20 % led to strength development of the AAC, but part of Al powder and lime did not react properly, because all mixes had the same water content (Fig. 12d). For AAC with 30 %SF, the CSH phase's improvement may be observed, as fibrous groups are surrounded by aggregate particles (Fig. 12e) and its porosity decreases with the addition of more SF.

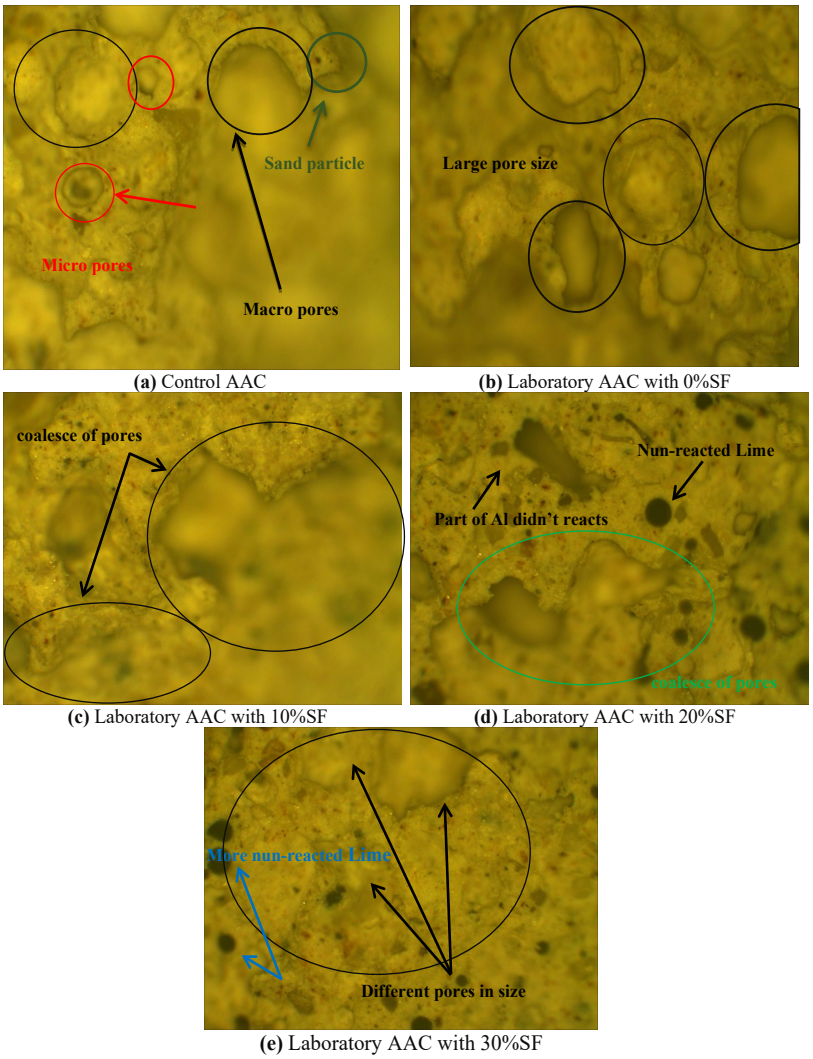

(a) Control AAC **(b)** Laboratory AAC with 0%SF

(c) Laboratory AAC with 10%SF **(d)** Laboratory AAC with 20%SF

(e) Laboratory AAC with 30%SF

Figure 12. Fracture surface micrographs for the control and experimental AAC samples with varying SF content.

4. Conclusion

The use of SF in autoclaved aerated concrete (AAC) has an eco-friendly effect in reducing the amount of waste material, and significantly influencing the physical and mechanical properties of AAC by improving the microstructure of the paste matrix. A series of AAC mixes with different content of SF (0–30 %) was created. At the end of the tests, the following results were obtained:

1. The effect of both lime to cement and sand to cement ratios was small, whereas the water to cement ratio had a considerable influence on the bulk density and compressive strength of AAC.

2. The compressive strength increased up to 6 times for the mixture containing up to 30 % of SF. The result showed that the progress of hydration reactions effects not only AAC strength but also pores filling with the hydration products.
3. It was indicated that an increase in pozzolanic materials resulted in increasing the tensile strength of the AAC sample. At the ratios of 10, 20 and 30 % SF, it was observed that the addition of SF up to 30 % slightly improved its tensile strength (approximately by 7 %). In addition, the brittleness of AAC was reduced by the addition of SF to increase strength. However, a considerable improvement in flexural strengths of AAC was obtained by using SF. 30 % of SF demonstrated high strength values of an adopted AAC sample, 3 times compared with that used in practical applications.
4. The maximum hardened density was with 30 % of SF, which was 54 % higher than that of the control sample, as it was affected by hardened density and its microstructure. The addition of SF resulted in improvement in tobermorite crystals and the pore structure of the AAC. Most of the air voids are unconnected voids, which were significantly affected by the introduction of SF. Due to the close relations between material properties and mix proportions, optimization of its proportions had great importance for the load-bearing strength of AAC.
5. SF caused a reduction in surface water absorption of AAC. The lowest water absorption was with 0 % SF that was reduced by 94 %, 28 % and 25 % respectively after 10, 30 and 90 min. However, the maximum water absorption of the proposed AAC was with 10 % of SF. It is recommended to use cementitious systems (SF + cement) to enhance the desired properties of AAC containing a high silica percentage. Moreover, additional research may be required on the influence of silica when taking into consideration the use of industrial wastes as adding/replacement materials in AAC production with varying percentages.

References

1. Qu, X., Zhao, X. Previous and present investigations on the components, microstructure and main properties of autoclaved aerated concrete – A review. Construction and Building Materials. 2017. 135. Pp. 505–516. DOI: 10.1016/j.conbuildmat.2016.12.208
2. Thienel, K.-C., Haller, T., Beuntner, N. Lightweight Concrete—From Basics to Innovations. Materials. 2020. 13(5). 1120. DOI: 10.3390/ma13051120
3. Sari, K., Sani, A.R. Applications of Foamed Lightweight Concrete. MATEC Web of Conferences. 2017. 97. 01097. DOI: 10.1051/matecconf/20179701097
4. Junaid, M.F., Rehman, Z.ur., Kuruc, M., Medveď, I., Bačinskas, D., Čurpek, J., et al. Lightweight concrete from a perspective of sustainable reuse of waste byproducts. Construction and Building Materials. 2022. 319. 126061. DOI: 10.1016/j.conbuildmat.2021.126061
5. Kalpana, M., Mohith, S. Study on autoclaved aerated concrete: Review. Materials Today: Proceedings. 2020. 22. Pp. 894–896. DOI: 10.1016/j.matpr.2019.11.099
6. Cai, Q., Ma, B., Jiang, J., Wang, J., Shao, Z., Hu, Y., et al. Utilization of waste red gypsum in autoclaved aerated concrete preparation. Construction and Building Materials. 2021. 291. 123376. DOI: 10.1016/j.conbuildmat.2021.123376
7. Wang, C.-l., Ni, W., Zhang, S.-Q., Wang, S., Gai, G.-S., Wang, W.-K. Preparation and properties of autoclaved aerated concrete using coal gangue and iron ore tailings. Construction and Building Materials. 2016. 104. Pp. 109–115. DOI: 10.1016/j.conbuildmat.2015.12.041
8. Mostafa, N.Y. Influence of air-cooled slag on physicochemical properties of autoclaved aerated concrete. Cement and Concrete Research. 2005. 35(7). Pp. 1349–1357. DOI: 10.1016/j.cemconres.2004.10.011
9. Kunchariyakun, K., Asavapisit, S., Sombatsompop, K. Properties of autoclaved aerated concrete incorporating rice husk ash as partial replacement for fine aggregate. Cement and Concrete Composites. 2015. 55. Pp. 11–16. DOI: 10.1016/j.cemconcomp.2014.07.021
10. Cai, L., Ma, B., Li, X., Lv, Y., Liu, Z., Jian, S. Mechanical and hydration characteristics of autoclaved aerated concrete (AAC) containing iron-tailings: Effect of content and fineness. Construction and Building Materials. 2016. 128. Pp. 361–372. DOI: 10.1016/j.conbuildmat.2016.10.031
11. Cai, L., Li, X., Liu, W., Ma, B., Lv, Y. The slurry and physical-mechanical performance of autoclaved aerated concrete with high content solid wastes: Effect of grinding process. Construction and Building Materials. 2019. 218. Pp. 28–39. DOI: 10.1016/j.conbuildmat.2019.05.107
12. Wongkeo, W., Thongsanitgarn, P., Pimraksa, K., Chaipanich, A. Compressive strength, flexural strength and thermal conductivity of autoclaved concrete block made using bottom ash as cement replacement materials. Materials & Design. 2012. 35. Pp. 434-439. DOI: 10.1016/j.matdes.2011.08.046
13. Różycka, A., Pichór, W. Effect of perlite waste addition on the properties of autoclaved aerated concrete. Construction and Building Materials. 2016. 120. Pp. 65–71. DOI: 10.1016/j.conbuildmat.2016.05.019
14. Gunasekaran, M., Elamaran, L., Suresh, P., Sakthivel, P., Saranya, G. Development of Light Weight Concrete by using Autoclaved Aerated Concrete. International Journal for Innovative Research in Science & Technology. 2016. 11(2). 5. Pp. 518–522.
15. Qin, L., Gao, X. Recycling of waste autoclaved aerated concrete powder in Portland cement by accelerated carbonation. Waste Management. 2019. 89. Pp. 254–264. DOI: 10.1016/j.wasman.2019.04.018
16. Li, X., Liu, Z., Lv, Y., Cai, L., Jiang, D., Jiang, W., et al. Utilization of municipal solid waste incineration bottom ash in autoclaved aerated concrete. Construction and Building Materials. 2018. 178. Pp. 175-182. DOI: 10.1016/j.conbuildmat.2018.05.147

17. Kunchariyakun, K., Asavapisit, S., Sinyoung, S. Influence of partial sand replacement by black rice husk ash and bagasse ash on properties of autoclaved aerated concrete under different temperatures and times. Construction and Building Materials. 2018. 173. Pp. 220–227. DOI: 10.1016/j.conbuildmat.2018.04.043
18. Zafar, M.S., Javed, U., Khushnood, R.A., Nawaz, A., Zafar, T. Sustainable incorporation of waste granite dust as partial replacement of sand in autoclave aerated concrete. Construction and Building Materials. 2020. 250. 118878. DOI: 10.1016/j.conbuildmat.2020.118878
19. Chen, Y.-L., Chang, J.-E., Lai, Y.-C., Chou, M.-I. A comprehensive study on the production of autoclaved aerated concrete: Effects of silica-lime-cement composition and autoclaving conditions. Construction and Building Materials. 2017. 153. Pp. 622–629. DOI: 10.1016/j.conbuildmat.2017.07.116
20. Pehlivanlı, Z.O., Uzun, İ., Demir, İ. Mechanical and microstructural features of autoclaved aerated concrete reinforced with autoclaved polypropylene, carbon, basalt and glass fiber. Construction and Building Materials. 2015. 96. Pp. 428–433. DOI: 10.1016/j.conbuildmat.2015.08.104
21. Pehlivanlı, Z.O., Uzun, İ., Yücel, Z.P., Demir, İ. The effect of different fiber reinforcement on the thermal and mechanical properties of autoclaved aerated concrete. Construction and Building Materials. 2016. 112. Pp. 325–330. DOI: 10.1016/j.conbuildmat.2016.02.223
22. Güçlüer, K., Ünal, O., Demir, İ., Başpınar, M.S. An Investigation of Steam Curing Pressure Effect on Pozzolan Additive Autoclaved Aerated Concrete. TEM Journal. 2015. 4. Pp. 78–82.
23. Zhao, Z., Qu, X., Li, F., Wei, J. Effects of steel slag and silica fume additions on compressive strength and thermal properties of lime-fly ash pastes. Construction and Building Materials. 2018. 183. Pp. 439–450. DOI: 10.1016/j.conbuildmat.2018.05.220
24. Leontev, S., Saraykina, K., Golubev, V., Yakovlev, G., Rakhimova, N., Shamanov, V., et al. Research into Influence of Ultra- and Nanodisperse Size Additives on the Structure and Properties of Heat Insulating Autoclaved Aerated Concrete. Procedia Engineering. 2018. 172. Pp. 649–656. DOI: 10.1016/j.proeng.2017.02.076
25. Pachideh, G., Gholhaki, M., Moshtagh, A. On the post-heat performance of cement mortar containing silica fume or Granulated Blast- Furnace Slag. Journal of Building Engineering. 2019. 24. 100757. DOI: 10.1016/j.jobe.2019.100757
26. Almajeed, I., Turki, S. Enhance Properties of Autoclaved Aerated Concrete by Adding Silica Fume. International Journal of Recent Technology and Engineering. 2019. 7(6). Pp. 11–15.
27. Lashari, A.R., Kumar, A., Kumar, R., Rizvi, S.H. Combined effect of silica fume and fly ash as cementitious material on strength characteristics, embodied carbon, and cost of autoclave aerated concrete. Environmental Science and Pollution Research. 2023. 30(10). Pp. 27875–27883. DOI: 10.1007/s11356-022-24217-9
28. IOS. Iraqi Organization of Standards, 5: Portland Cement. National Centre for Construction Laboratories and Researches, 2019.
29. IOS. Iraqi Organization of Standards, 45-84 (Reapproved 2016): Aggregates from Natural Sources for Concrete and Construction. . National Centre for Construction Laboratories and Researches, 2016.
30. ECA. ECA® MICROSILICA-D. Amman - Jordan: Europen concrete additives, 2010.
31. IOS. Iraqi Organization of Standards, 807: Lime Using in Construction. National Centre for Construction Laboratories and Researches, 1988.
32. ACI-Committee. ACI-2349: Guide for the use of silica fume in concrete. USA: American Concrete Institute, 2000. Pp. 1-63.
33. BS-EN. BS EN 679: Determination of the compressive strength of autoclaved aerated concrete, 2005.
34. BS-EN. BS EN 1881-117: Testing concrete. Method for determination of tensile splitting strength, 1983.
35. BS-EN. BS EN 1351: Determination of flexural strength of autoclaved aerated concrete, 1997.
36. BS-EN. BS EN 678: Determination of the dry density of autoclaved aerated concrete. 94th ed2017 1 June 2017.
37. Al-Defai, N. The consequences of the dewatering of freshly-mixed wet mortars by the capillary suction of brick masonary. University of Manchester, 2013.
38. BS-EN. BS EN 772-11: Methods of test for masonry units. Determination of water absorption of aggregate concrete, autoclaved aerated concrete, manufactured stone and natural stone masonry units due to capillary action and the initial rate of water absorption of clay masonry units: British Standards Institution (BSI), 2011.
39. ASTM. ASTM C1639: Standard specification for fabrication of cellular glass pipe and tubing insulation. The American Society for Testing and Materials, 2019. 4 p.
40. Link to the Figure 5 https://www.mtixtl.com/advancedmetallurgicalmicroscopewithpolarizingdarkfieldandduallights30mpdigitalcamera40x-1600x-eq-mm500t-usb.aspx.
41. Naik, T.R. Concrete durability as influenced by density and/or porosity. Cement and Concrete Institute of Mexico Symposium "World of Concrete - Mexico": Milwaukee DoCEaMCoEaASTUOW; 1997.
42. Rathod, S., Akbari, Y. Performance evaluation of aerated autoclaved concrete blocks using silica fume. Journal of Emerging Technologies and Innovative Research (JETIR). 2017. 4(4). Pp. 220-225.
43. ASTM. ASTM C1693-11: Standard Specification for Autoclaved Aerated Concrete (AAC). The American Society for Testing and Materials, 2017.
44. Pachideh, G., Gholhaki, M. Effect of pozzolanic materials on mechanical properties and water absorption of autoclaved aerated concrete. Journal of Building Engineering. 2019. 26. 100856. DOI: 10.1016/j.jobe.2019.100856
45. Wan, H., Hu, Y., Liu, G., Qu, Y. Study on the structure and properties of autoclaved aerated concrete produced with the stone-sawing mud. Construction and Building Materials. 2018. 184. Pp. 20–26.
46. Toutanji, H.A., Liu, L., El-Korchi, T. The role of silica fume in the direct tensile strength of cement-based materials. Materials and Structure. 1999. 32. 7. DOI: 10.1007/BF02481516
47. Baspinar, M., Demir, I., Kahraman, E., Gorhan, G. Utilization Potential of Fly Ash together with Silica Fume in Autoclaved Aerated Concrete Production. KSCE Journal of Civil Engineering. 2014. 18(1). Pp. 47–52. DOI: 10.1007/s12205-014-0392-7
48. Thongtha, A., Maneewan, S., Punlek, C., Ungkoon, Y. Investigation of the compressive strength, time lags and decrement factors of AAC-lightweight concrete containing sugar sediment waste. Energy and Buildings. 2014. 84. Pp. 516–525. DOI: 10.1016/j.enbuild.2014.08.026

49. Narayanan, N., Ramamurthy, K. Structure and properties of aerated concrete: a review. Cement and Concrete Composites. 2000. 22(5). Pp. 321–329. DOI: 10.1016/s0958-9465(00)00016-0
50. Elrahman, M.A., Chung, S.-Y., Sikora, P., Rucinska, T., Stephan, D. Influence of Nanosilica on Mechanical Properties, Sorptivity, and Microstructure of Lightweight Concrete. Materials. 2019. 12(19). 3078. DOI: 10.3390/ma12193078
51. Mindess, S., Young, J., Darwin, D. Concrete. 2nd ed. U.S.A.: Prentice Hall, Pearson Education, Inc. Upper Saddle River, NJ 07458, 2003.

Information about the author:

Rana Shabbar
ORCID: https://orcid.org/0000-0003-3087-0333
E-mail: rana.shubber@uokufa.edu.iq

Layth Abdulrasool Mahdi Alasadi,

ORCID: https://orcid.org/0000-0001-6244-7965

E-mail: laitha.alasadi@uokufa.edu.iq

Jaber Kadhim Taher,

Received: 14.02.2023. Approved after reviewing: 14.11.2023. Accepted: 17.11.2023.